




Research Article

Resident memory CD4⁺ T lymphocytes mobilize from bone marrow to contribute to a systemic secondary immune reaction

Carla Cendón^{\$1}, Weijie Du^{§,†1}, Pawel Durek^{#1}, Yuk-Chien Liu^{#1}, Tobias Alexander², Lindsay Serene³, Xinyi Yang⁴, Gilles Gasparoni⁵, Abdulrahman Salhab⁵, Karl Nordström^{##5}, Tina Lai¹, Axel R. Schulz⁶, Anna Rao¹, Gitta A. Heinz⁷, Ana L. Stefanski², Anne Claußnitzer², Katherina Siewert⁸, Thomas Dörner², Hyun-Dong Chang^{1,9} , Hans-Dieter Volk^{10,11}, Chiara Romagnani^{12,13}, Zhihai Qin^{14,15}, Sebastian Hardt¹⁶, Carsten Perka¹⁶, Simon Reinke¹¹, Jörn Walter⁵, Mir-Farzin Mashreghi^{7,11}, Kevin Thurley^{‡,§\$17,18}, Andreas Radbruch^{*1}  and Jun Dong^{*1} 

¹ Cell Biology, Deutsches Rheuma-Forschungszentrum Berlin (DRFZ), Institute of the Leibniz Association, Berlin, Germany

² Department of Rheumatology and Clinical Immunology, Charité-Universitätsmedizin Berlin, Berlin, Germany

³ Department of Biological Sciences, University of Notre Dame, Notre Dame, Indiana, USA

⁴ Otto-Warburg-Laboratory, Computational Epigenomics, Max Planck Institute for Molecular Genetics, Berlin, Germany

⁵ Department of Genetics, University of Saarland (UdS), Saarbrücken, Germany

⁶ Mass Cytometry, Deutsches Rheuma-Forschungszentrum Berlin (DRFZ), Institute of the Leibniz Association, Berlin, Germany

⁷ Therapeutic Gene Regulation, Deutsches Rheuma-Forschungszentrum Berlin (DRFZ), Institute of the Leibniz Association, Berlin, Germany

⁸ Department of Chemical and Product Safety, German Federal Institute for Risk Assessment, Berlin, Germany

⁹ Schwiete-Laboratory for Microbiota and Inflammation, Deutsches Rheuma-Forschungszentrum Berlin (DRFZ), Institute of the Leibniz Association, Berlin, Germany

¹⁰ Institute for Medical Immunology, Charité-Universitätsmedizin Berlin, Berlin, Germany

¹¹ BIH Center for Regenerative Therapies (BCRT), Charité-Universitätsmedizin Berlin, Berlin, Germany

¹² Innate Immunity, Deutsches Rheuma-Forschungszentrum Berlin (DRFZ), Institute of the Leibniz Association, Berlin, Germany

¹³ Medical Department/Gastroenterology, Infectiology and Rheumatology, Charité-Universitätsmedizin Berlin, Berlin, Germany

¹⁴ Key Laboratory of Protein and Peptide Pharmaceuticals, Institute of Biophysics, Chinese Academy of Sciences, Beijing, P. R. China

¹⁵ Medical Research Center, The First Affiliated Hospital of Zhengzhou University, Zhengzhou University, Zhengzhou, P. R. China

¹⁶ Center for Musculoskeletal Surgery, Charité-Universitätsmedizin Berlin, Berlin, Germany

¹⁷ Systems Biology of Inflammation, Deutsches Rheuma-Forschungszentrum Berlin (DRFZ), Institute of the Leibniz Association, Berlin, Germany

¹⁸ Institute for Theoretical Biology, Humboldt University, Berlin, Germany

^{\$}Carla Cendón and Weijie Du contributed equally to this work.

[†]Current affiliation: Berlin Center for Advanced Therapies (BeCAT), Charité-Universitätsmedizin Berlin, Berlin, Germany.

[‡]Current affiliation: Institute for Experimental Oncology, Biomathematics division, University Hospital Bonn.

[#]Pawel Durek and Yuk-Chien Liu contributed equally to this work.

^{##}Currently employed by AstraZeneca.

^{*}Andreas Radbruch and Jun Dong share the joint final authorship.

^{\$§}Correspondence for Bioinformatics; email: kevin.thurley@uni-bonn.de

Correspondence: Jun Dong
e-mail: dong@drfz.de

Resident memory T lymphocytes (T_{RM}) of epithelial tissues and the Bm protect their host tissue. To what extent these cells are mobilized and contribute to systemic immune reactions is less clear. Here, we show that in secondary immune reactions to the measles-mumps-rubella (MMR) vaccine, $CD4^+ T_{RM}$ are mobilized into the blood within 16 to 48 h after immunization in humans. This mobilization of T_{RM} is cognate: T_{RM} recognizing other antigens are not mobilized, unless they cross-react with the vaccine. We also demonstrate through methylome analyses that T_{RM} are mobilized from the Bm. These mobilized cells make significant contribution to the systemic immune reaction, as evidenced by their T-cell receptor V β clonotypes represented among the newly generated circulating memory T-cells, 14 days after vaccination. Thus, T_{RM} of the Bm confer not only local, but also systemic immune memory.

Keywords: Bm Trm cells · epigenetic signature · mobilization · systemic memory · T-cell receptor repertoire



Additional supporting information may be found online in the Supporting Information section at the end of the article.

Introduction

Recent research has provided compelling evidence that, in addition to circulating central memory T cells (T_{CM}) and effector memory T cells (T_{EM}), which are readily detectable in the blood at all times [1], there are also significant populations of noncirculating, tissue-resident memory T lymphocytes (T_{RM}). T_{RM} have been described for a variety of tissues, such as the skin, gut, lungs, liver [2–6], and Bm [7–11]. Compartments of T_{RM} have been defined by confinement in parabiosis experiments [12, 13], by distinct gene expression signatures, including the marker CD69 [4, 7, 11, 14–16], and by exclusive antigen receptor repertoires and specificities [3, 7, 11]. While T_{RM} of epithelial tissue are capable of providing enhanced local protection at sites of previous infections [2, 3, 13, 17–20], T_{RM} of Bm preferentially maintain long-term memory for systemic pathogens, like measles, mumps, and rubella viruses. In elderly individuals with high titers of measles-specific antibodies, few, if any, measles-specific memory $CD4^+$ T lymphocytes are detectable in the blood, but they are readily detectable in the Bm [7]. The question is: Do these cells also contribute to systemic immune reactions?

Memory T cells are epigenetically imprinted to rapidly (re)express, that is, “memorize” distinct genes upon reactivation of their antigen-receptor, such as the *IFNG* gene for Th1 cells [21], the *IL4* gene for Th2 cells [22], and the *RORC2*, *IL17A*, and *IL17F* genes for both Th17 and Th17-derived Th1 cells [23]. In addition, global demethylation of DNA accompanies proliferation and differentiation of memory T cells, with T_{CM} (central memory), T_{EM} (effector memory), and T_{EMRA} (T_{EM} cells reexpressing CD45RA) of blood showing a distinct pattern of demethylation which progresses along the line of differentiation, while Bm-resident $CD4^+$ memory T cells show a different pattern of global demethylation [24].

In the Bm of humans and mice, T_{RM} reside individually and rest in niches organized by stromal cells, nonproliferative, and

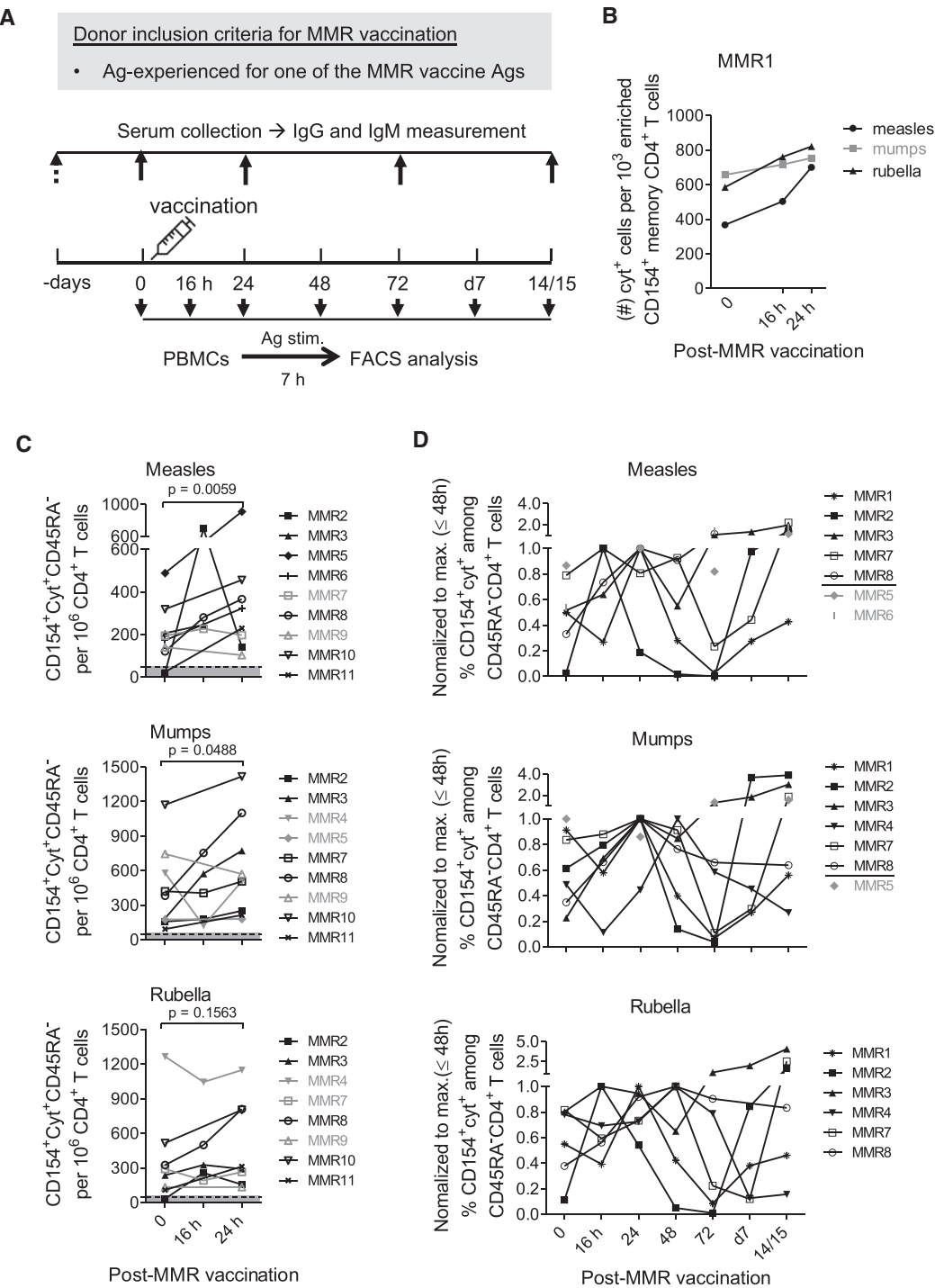
transcriptionally silent [7, 8, 11]. Upon reactivation by antigen, murine $CD4^+ T_{RM}$ of the Bm form “immune clusters” and proliferate vigorously in the Bm, but GC-like structures are not observed there [25]. Upon adoptive transfer, T_{RM} of Bm can also contribute decisively to secondary immune reactions [11], and fate mapping of T_{RM} in mice has shown that memory T cells downstream of T_{RM} can contribute to secondary immune reactions, although the original tissue(s) of residency remained unclear [26, 27].

Here, we describe the cognate mobilization of human $CD4^+ T_{RM}$ into the blood, in reaction to a challenge with the live attenuated measles-mumps-rubella (MMR) vaccine, within 16 to 48 h after vaccination. Their epigenetic signature indicates mobilized T_{RM} as derived from the Bm. The mobilized T_{RM} then disappear again from the blood, and subsequently, their T-cell receptor (TCR) repertoire is included into the repertoire of newly generated, circulating memory T lymphocytes. Thus, Bm T_{RM} are rapidly mobilized and participate significantly in relevant secondary immune reactions to systemic antigens.

Results

Mobilization of $CD4^+ T_{RM}$ into the blood in a secondary immune response

Eleven healthy human volunteers (MMR1-11), aged 28 to 43 years, were immunized subcutaneously with the live attenuated MMR virus vaccine, as outlined in Fig. 1A. Prior to vaccination, serum IgG titers, specific for each of the three viruses, had been determined to reassure their pre-existing memory. Except vaccinee MMR4, who lacked antibodies specific for the measles virus, all vaccinees had antibodies specific for each of the three viruses, prior to vaccination (Supporting information Table S1). Virus-reactive memory $CD4^+$ T lymphocytes were identified upon restimulation with antigen ex vivo, as cells expressing CD154



(CD40L) and one or more of the cytokines IL-2, TNF- α , and IFN- γ , as described previously [7, 28] (Supporting information Fig. S1A and B), at the time points indicated in Fig. 1A. Frequencies of antigen-reactive memory CD4⁺ T lymphocytes were highly reproducible between measurements for technical replicates (Supporting information Fig. S2A) as well as for biological replicates, that is, blood samples from individual control donors, taken on two consecutive days without vaccination (Supporting information Fig. S2B).

To examine the kinetics of antigen-reactive memory CD4⁺ T cells in response to vaccination, we monitored the levels of 29 virus-reactive memory CD4⁺ T-cell responses over time for measles (in 11 vaccinees), mumps (10 vaccinees), and rubella (9 vaccinees). Strikingly, vaccine-reactive memory CD4⁺ T cells were rapidly mobilized into the blood in most, though not all vaccinees, evident from a significant increase in the number of memory CD4⁺ T cells reactive to measles (average from 188 to 344 per 10⁶ CD4⁺ T cells) and mumps (average from 416 to 627 per 10⁶ CD4⁺ T cells), within 16 to 24 h after vaccination (Fig. 1B and C). By 24 h postvaccination, differences in the frequencies of measles-, mumps-, and rubella-reactive memory CD4⁺ T cells in the blood increased significantly, as compared to time-matched “baseline” controls of not vaccinated donors (Supporting information Fig. S2C).

Twenty of the 29 memory T-cell responses were also analyzed at 48- and/or 72-h after vaccination. Of those, 17 showed peak responses of virus-specific CD154⁺cytokine⁺ memory CD4⁺ T cells at 16-, 24-, or 48-h after vaccination, followed by a steep drop in frequencies (Fig. 1D), and in numbers to baseline or below (Supporting information Fig. S3A) by 3–4 days. For example, a 37-fold increase in frequency (Fig. 1D) of measles-reactive memory CD4⁺ T cells corresponding to 676 more cells per 10⁶ CD4⁺ T cells were observed at 16-h after vaccination in vaccinee MMR2 (Supporting information Fig. S3A). Similar early peak responses of memory CD4⁺ T-cells reactive to the three vaccine antigens are also exemplified by vaccinees MMR3 and MMR8 (Supporting information Fig. S3A). Taken together, these data indicate that antigen-reactive T_{RM} are rapidly mobilized from their tissues of residence and into circulation upon reactivation, and then disappear again from the blood.

We continued tracking antigen reactive CD4⁺ T cells till day 14 after vaccination. In 26 of the 29 immune reactions monitored, on average three- to fourfold increase in cell numbers (Supporting information Fig. S3B) and four- to tenfold increase in frequencies (Fig. 1D) of virus-reactive circulating memory T cells were detected on day 14, as compared to d0 prevaccination levels. It is

interesting to note that among these 26 memory T-cell responses analyzed, only 13 also showed an increase in virus-specific serum IgG antibody titers (Supporting information Fig. S3A), and that the magnitude of memory T-cell responses 2 weeks after vaccination did not significantly correlates with specific antibody titers before vaccination (Supporting information Fig. S4).

Mobilized T_{RM} are activated, nonproliferative, and polyreactive

In accordance with the rapid mobilization of vaccine-specific T_{RM}, as defined by their reaction to the antigens *ex vivo* (Supporting information Fig. S1A and B), we also detected a rapid mobilization of *in vivo* activated memory T cells in the four vaccinees analyzed (MMR2, MMR3, MMR7, and MMR8) 16 to 48 h after vaccination. Without restimulation *ex vivo*, these cells expressed CD154 (Fig. 2A) and cytokines like IL-2, IFN- γ , or TNF- α (Fig. 2B).

It is a matter of debate whether memory T cells, tissue-resident, or circulating, are maintained as nonproliferative, resting cells. To examine mobilized vaccine-specific memory CD4⁺ T cells for their ability to proliferate, these cells were stained for expression of Ki67, an antigen that is expressed in all the phases of the cell cycle, except for G₀ [29]. Here, we show that the numbers of Ki-67⁺ expressing virus-reactive memory T cells were undetectable in the blood of vaccinees up to 72 h after vaccination (Fig. 2C; Supporting information Fig. S5), implying that mobilized memory T cells are nonproliferative. Later, on days 7 and 14 after reimmunization, antigen-reactive Ki-67⁺CD154⁺cytokine⁺ memory CD4⁺ T cells were readily detectable in the blood (Fig. 2C; Supporting information Fig. S5), apparently reflecting newly generated effector or memory cells.

In secondary immune responses to infectious pathogens, such as viruses, activated memory CD4⁺ T cells with the coexpression of two or more of the cytokines IL-2, IFN- γ , and TNF- α , are considered to be more protective than those expressing only one of the three cytokines [30, 31]. In contrast to circulating memory T cells, T_{RM}, especially measles-reactive memory CD4⁺ T cells residing in the Bm, have been shown to express several cytokines simultaneously upon reactivation [7]. Here, we show that upon MMR revaccination, in 19 out of 29 memory T-cell responses with mobilized memory CD4⁺ T cells, the majority of the CD4⁺ T cells, peaking on day 1 express several cytokines simultaneously, that is, they are “polyfunctional” (Fig. 2D; Supporting information Fig. S6A–C) [30].

Figure 1. Mobilization of CD4⁺ T_{RM} into the blood in a secondary immune response. (A) Donor inclusion criteria and scheme for analyzing virus-specific memory CD4⁺ T-cell responses following MMR booster vaccination. PBMCs from 11 vaccinees were stimulated with measles, mumps, or rubella and analyzed for antigen-reactive CD154⁺cytokine⁺ memory T cells (memory CD4⁺ T-cells expressing CD154 [CD40L] and one or more of the cytokines IL-2, TNF- α , and IFN- γ) per 10³ enriched CD154⁺ memory CD4⁺ T cells (B; MMR1) or per 10⁶ CD4⁺ T cells (C; MMR2–11) and in frequencies relative to its maximum by 48 h after vaccination (D) at the indicated time points. In C, the dotted black line indicates the minimum threshold for detection for the assay and the grey area underneath indicates values below the reliable detection limit. Significance was determined using paired t-test with Welch's correction. One-tailed *p* values are reported. In both B and C, data shown in grey represent the responses at 24-h that are less than 30% greater than those before vaccination. In D, data shown in grey indicate vaccinees analyzed at the following time points: before (0), 24-, 72-h, and 2 weeks after vaccination. In B–D, data shown from indicated vaccinee(s) are representative of 55 independent experiments.

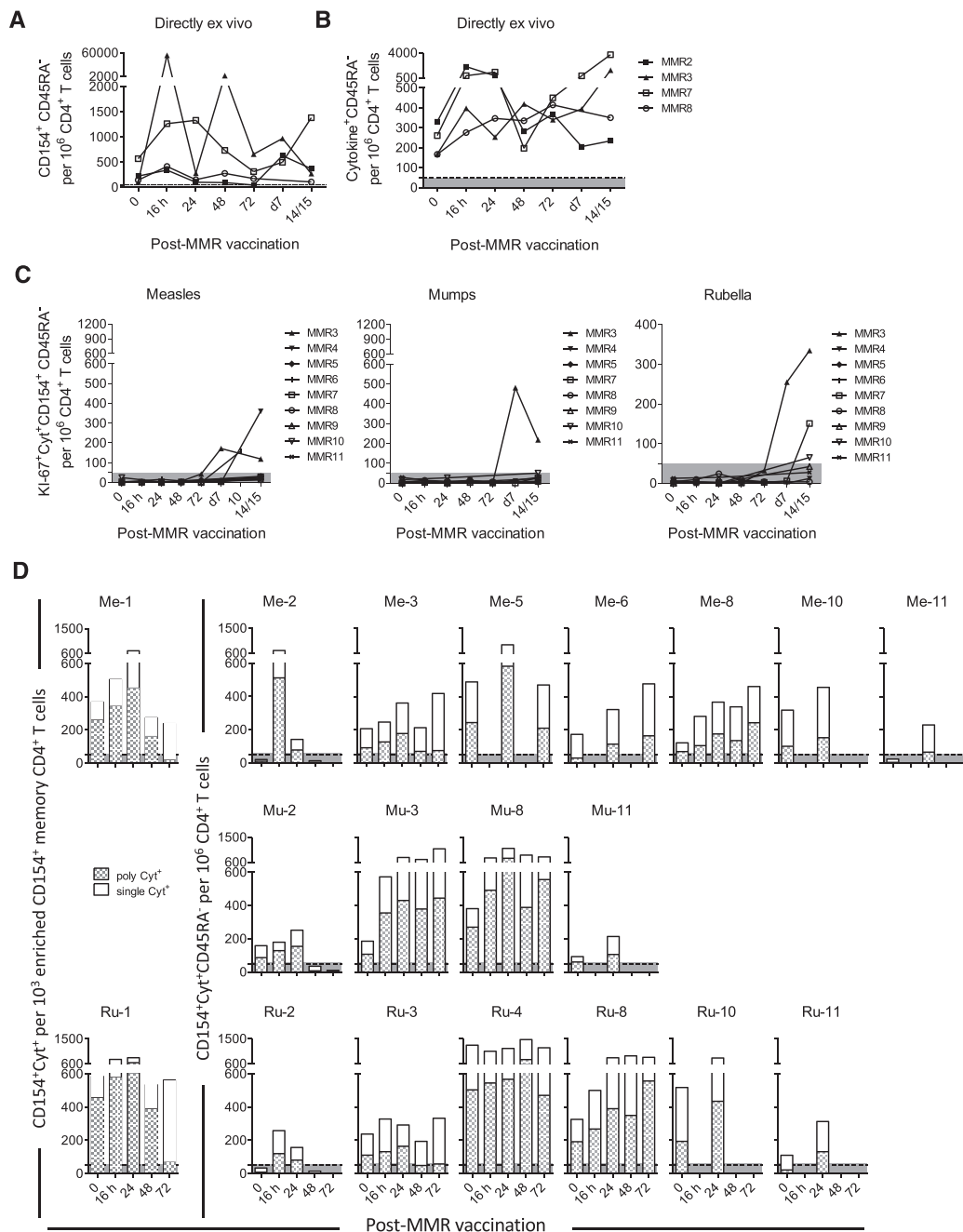


Figure 2. Mobilized T_{RM} are activated, non-proliferative and polyreactive. (A) PBMCs from vaccinees analyzed immediately after isolation for CD154⁺ (A) and CD154⁺cytokine⁺ (B) CD45RA⁻ memory T cells per 10⁶ CD4⁺ T cells before and at indicated time points after vaccination. (C, D) PBMCs from vaccinees stimulated with measles, mumps, or rubella and analyzed for antigen-reactive Ki-67⁺CD154⁺cytokine⁺ memory T cells (C) and single, double, or triple cytokine-producing subpopulations of CD154⁺cytokine⁺ memory T cells (D) per 10⁶ CD4⁺ T cells before and at indicated time points after vaccination. In C and D, the dotted black line marks the assay's minimum threshold for detection, and the grey areas underneath represent values below the reliable limit of detection. In A–D, data shown from indicated vaccinees are representative of at least 20 independent experiments.

Mobilization of CD4⁺ T_{RM} by MMR vaccine is cognate

The rapid mobilization of vaccine-reactive memory CD4⁺ T cells into the blood was not due to a general increase in the numbers of peripheral T cells and memory T cells (Supporting information Fig. S7). To determine whether the rapid mobilization of vaccine-

reactive memory T cells is antigen-specific or not, we determined whether the MMR vaccine also mobilized memory T cells recognizing the antigen tetanus toxoid (TT). Surprisingly, we observed a rapid mobilization of TT-reactive memory T cells in three out of four vaccinees analyzed (Fig. 3A). Moreover, these vaccinees also showed a drop in numbers of TT-reactive memory T cells on

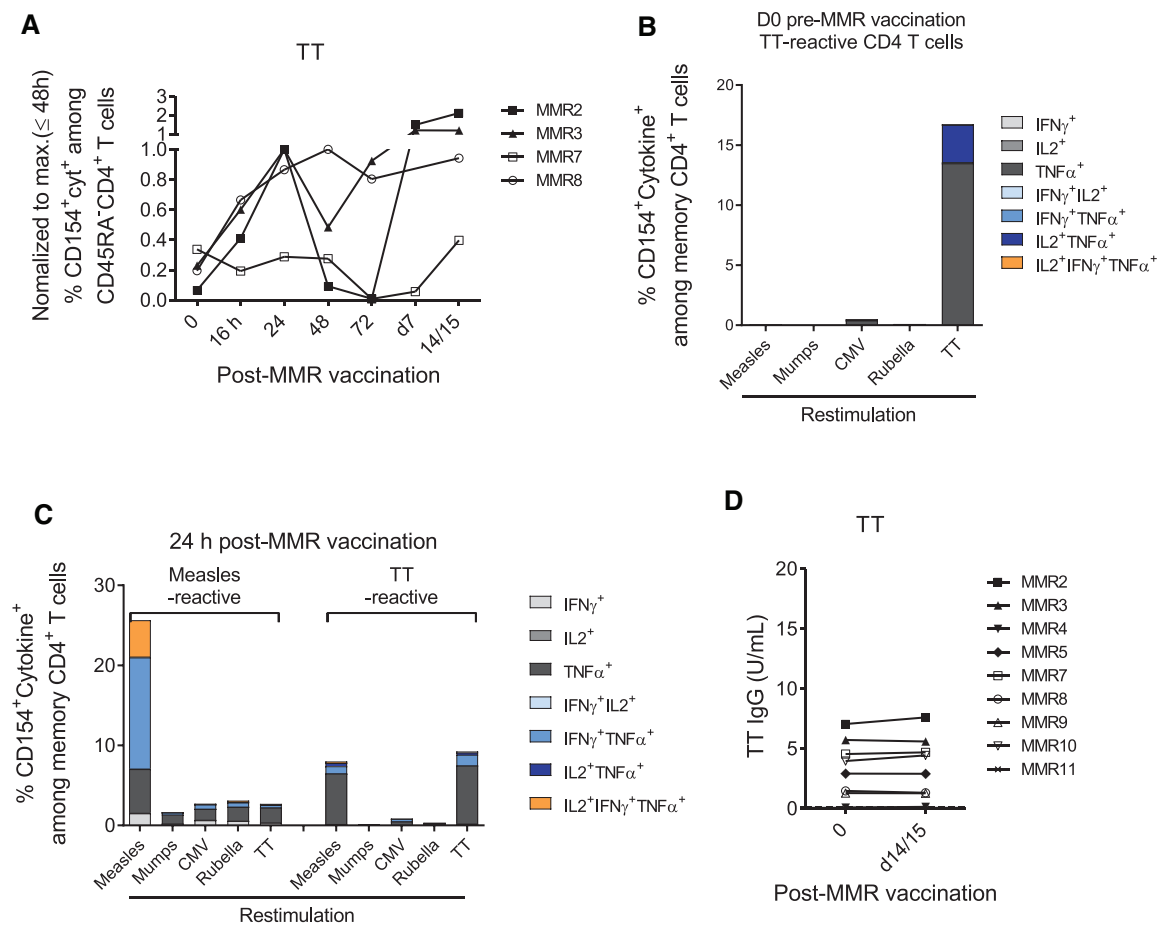


Figure 3. Mobilized CD4⁺ T_{RM} by MMR vaccine is cognate. (A) Mobilization of TT-reactive memory T cells following MMR booster vaccination. PBMCs from four vaccinees stimulated with TT and analyzed for TT-reactive CD154⁺cyt⁺ CD45RA⁻ memory CD4⁺ T cells. (B, C) Specificity of expanded measles- or TT-reactive CD154⁺ memory CD4⁺ T cell lines isolated before (B) after (C) MMR vaccination. PBMCs from MMR vaccinees MMR8 were stimulated with measles antigen or TT before (d0; B) or one (d1; C) day after MMR vaccination. Antigen-reactive CD154⁺ CD4⁺ memory T cells were isolated from these samples and expanded for 14 days with IL-2 and autologous antigen-presenting cells. Expanded cell lines were then restimulated with the indicated antigens in the presence of autologous antigen-presenting cells and reactive cells were identified by coexpression of CD154 and one or more of the cytokines: IL-2, TNF- α , and/or IFN- γ . (D) The production of IgG antibodies specific for TT antigen before and after MMR vaccination for indicated vaccinees. The dotted black line marks the assay's minimum threshold for detection, and the grey area underneath represents values below the reliable limit of detection. (A–D) Data shown are representative of at least three independent experiments.

days 2 and/or 3 following vaccination, and their reappearance again between days 7 and 14 (Fig. 3A), resembling the kinetics of vaccine-reactive memory T cells (Supporting information Fig. S3A). One of the donors (MMR7) did not show a mobilization of TT-reactive memory T cells, demonstrating that no such T_{RM} had been pre-existing in that donor, and serving as an important internal control, demonstrating the specificity of mobilization.

To investigate whether the mobilized TT-reactive memory T cells were cross-reactive to the MMR vaccine, TT-reactive CD154⁺CD69⁺ memory T cells were isolated from one vaccinee (MMR8) before and one day after MMR vaccination. These cells were then expanded for 2 weeks with IL-2, before restimulation with measles, mumps, rubella, CMV, or TT antigens. TT-reactive T cells isolated before vaccination were only reactive to TT, but not to other analyzed antigens (Fig. 3B). Interestingly, TT-reactive T cells isolated after vaccination were reactive to both TT and measles, but not to mumps or rubella (Fig. 3C), suggest-

ing that cross-reactive memory T cells had been mobilized in this vaccinee, and that mobilization indeed had been antigen-specific. Even though cross-reactive memory T cells were mobilized, and apparently also activated by MMR vaccination, this did not have a detectable impact on TT-specific serum antibody titers (Fig. 3D).

Mobilized CD4⁺ T_{RM} contribute to a systemic secondary immune reaction

To determine whether mobilized vaccine-reactive memory T cells contribute to the immune response triggered by the vaccine, we compared the TCR CDR3 V β clonotypes of rapidly mobilized memory T cells to those of the memory T cells present in the blood 14 days after vaccination. To this end, two replicates with equal numbers (2.5×10^3) of measles-reactive CD154⁺CD69⁺ memory CD4⁺ T cells (which include cytokine-secreting cells)

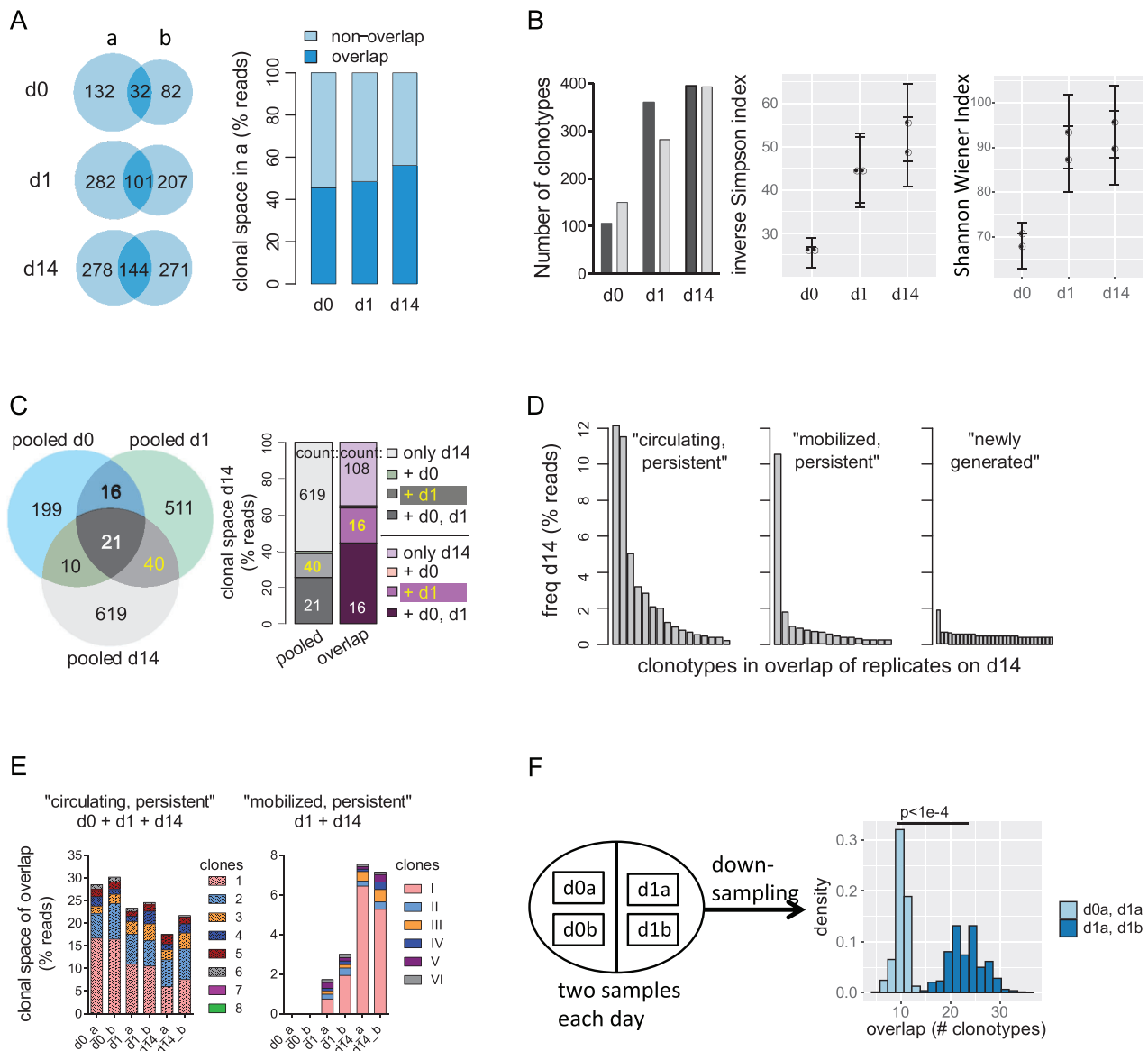


Figure 4. Mobilized CD4⁺ T_{RM} contribute to a systemic immune reaction. PBMCs that were isolated before (d0) and one (d1) and 14 (d14) days after MMR vaccination from vaccinee MMR10, were restimulated ex vivo with measles antigen, and examined for measles-reactive CD154⁺CD69⁺ memory CD4⁺ T cells. Analogous data for vaccinee MMR11 are shown in Supporting information Fig. S8. (A) Analysis from two replicates of CDR3 Vβ clonotypes for each time point show the “overlap,” that is, the number of clonotypes detected in both replicates, in clonotype count (Venn diagrams) and frequency (bar graphs). (B) TCR repertoire diversity was measured using the inverse Simpson and Shannon Wiener indices at three time points for both replicates in A. Error bars indicate standard deviation after repetitive down-sampling. (C) Venn diagrams show comparative numbers of clonotypes in “pooled” repertoires, that is, clonotypes detected in at least one replicate. Clonal space (bar graph) corresponds to the fraction of reads detected on d14, “overlap,” that is, clonotypes detected in at least one of the replicates at the indicated time points. Numbers in the bar plot indicate the numbers of clonotypes (for pooled replicates, these numbers match those of the Venn diagram). (D) Frequency distributions of “circulating, persistent” (d14 + d0 + d1), “mobilized, persistent” (d14 + d1), and “new” (only d14) clonotypes (see C), as compared to the clones in overlap of replicates on d14. For “new,” only the 30 most frequent clonotypes are shown. (E) Contribution of each replicate to the “circulating, persistent” and “mobilized, persistent” clonotypes. Clonal space is given as the percentage of reads in the overlap of replicates on indicated days, and only clonotypes present in all relevant samples are shown. (F) Comparison of the overlap of samples taken on different days or taken on the same day. Shown are the distributions of indicated sample overlaps after repetitive down-sampling to the smallest number of reads among all samples taken on d0 and d1 (see also Supporting information Fig. S8F).

were isolated from 30 mL of peripheral blood drawn from donors MMR10 and MMR11 before (d0), and one (d1) and 14 (d14) days after MMR vaccination. The global CDR3 Vβ clonal repertoires of measles-reactive memory CD4⁺ T cells at these three time points

(Fig. 4A; Supporting information Table S2, Fig. S8A) were then compared based on their clonal diversity and relatedness.

The number of CDR3 Vβ clonotypes increased by ≥75% from d0 to d1 in both vaccinees, MMR10 (Fig. 4B) and MMR11

(Supporting information Fig. S8B), as well as across all measured samples. Clonal diversity increased from d0 to d1 in both donors as well, as quantified by the inverse Simpson index, which provides a measure of diversity that can be interpreted as the “effective number of parties” in a given sample [32] (Fig. 4B; Supporting information Fig. S8B). By day 14, the diversity and number of clonotypes stayed high in MMR10 (Fig. 4A), and decreased to basal levels in MMR11 (Supporting information Fig. S8B), in line with their T-cell response kinetics (Supporting information Fig. S4B). Another measure of diversity, the Shannon Wiener Index (Fig. 4B; Supporting information Fig. S8B) gave qualitatively similar results. Together, these results demonstrate that the MMR vaccine triggers the mobilization of antigen-reactive memory CD4⁺ T cells expressing distinct clonotypes, which had been absent from the repertoire of pre-existing circulating memory T cells prior to vaccination.

To assess the contribution mobilized T cells make to the CDR3 V β clonotype repertoire on day 14 postvaccination, we analyzed the clonal space at this time in more detail. To this end, we considered both the “pooled” clonal space (clonotypes detected in either of the replicates) and the “overlapping” clonal space (clonotypes detected in both replicates) (Fig. 4A and C; Supporting information Fig. S8A and C). In both vaccinees, the largest fraction of antigen-reactive CD4⁺ T cells on day 14 consisted of clonotypes that had not been detected in the blood on either day 0 or day 1, 619 clonotypes comprised 60% of the pooled clonal space for MMR10, and 488 clonotypes comprised 80% of pooled clonal space for MMR11 (Fig. 4C). On day 14, 21 clonotypes represented in MMR10 and 22 in MMR11 (about 25% and 10% of the pooled clonal space, respectively) were identified as “circulating” clonotypes that were detected on d0, d1, and d14. At the same time, 40 clonotypes represented in MMR10 and 60 in MMR11 (comprising about 15% and 10% of the pooled clonal space, respectively) were identified as “mobilized” clonotypes, that is, detected on d1 and d14, but not on d0 (Fig. 4C; Supporting information Fig. S8C; highlighted in yellow). In the “overlapping” clonal space, representing clonotypes detected in both replicates of each day for a given vaccinee, the “mobilized” clonotypes represented about 20 and 10% of the repertoire on d14 for MMR10 and MMR11, respectively. Similarly, the “circulating” clonotypes at the same time point accounted for about 40 and 15% of the repertoire for donors MMR10 and MMR11, respectively (Fig. 4C; Supporting information Fig. S8C). Remarkably, we detected three highly abundant clonotypes with more than 5% of reads in donor MMR10, one characterized as “mobilized” and two “circulating” (Fig. 4D). In MMR11, no highly abundant clones were detected on d14 (Supporting information Fig. S8D), in agreement with the reduced Simpson diversity measured in this donor (Supporting information Fig. S8B). In both donors MMR10 and MMR11, individual “circulating” and “mobilized” clones that were consistently detectable in each of the replicates maintained their clonal space or even expanded, such as clone I of donor MMR10 (Fig. 4E; Supporting information Fig. S8E).

To exclude the option that detection of increased diversity on d1, as compared to d0, was merely due to the higher sampling rate on d1 (Supporting information Table S2), we tested the “null hypothesis” that the repertoires on d0 and d1 had the same number of different clonotypes. If that had been the case, and all samples taken on d0 and d1 were representing the same repertoire, only at varying sampling effectivity, the overlap between replicates on each day would be the same as those between replicates of different days. However, this is not the case: after repetitive random down sampling of the number of reads from a given sample to those with the least number, the distribution of those with overlapping regions between replicates of the same day was significantly different from the distribution of overlapping regions between replicates representing different days (Fig. 4F; Bonferroni corrected p -values $< 10^{-4}$). This was true for all possible combinations of samples in both donors, ruling out the null hypothesis (Supporting information Fig. S8F), and demonstrating that indeed the repertoires of d0 and d1 were different due to the mobilization of memory T cells with additional clonotypes.

Taken together, these findings show that MMR vaccination induced an influx of mobilized measles-specific CD4⁺ T_{RM} coexpressing functional new CDR3 V β clonotypes into the blood, establishing that mobilized T_{RM} provide a significant contribution to the systemic secondary immune reactions against measles.

T_{RM} are mobilized from Bm

T_{RM} could be derived from secondary lymphoid organs, or from tissues, which do not mount classical, GC-based secondary immune reactions themselves, like the Bm [25]†††. To identify the tissue-of-origin of the T_{RM} mobilized by vaccination, we analyzed their epigenetic signatures, which we had shown earlier to discriminate between circulating memory T cells from blood and T_{RM} of Bm [24], and which we considered to be robust against activation and mobilization of the T_{RM}. T_{RM} of spleen (Sp) and Bm, and antigen-reactive memory T cells from blood before vaccination (day 0) and on day 1 after vaccination, at the peak of mobilization, were submitted to multiplex reduced representative bisulfite sequencing (mRRBS) [33] (Supporting information Table S3). Measles- and TT-reactive memory CD4⁺ T cells were isolated *ex vivo* from the blood of two vaccinees before (d0) and one day (d1) after vaccination with MMR or diphtheria-tetanus-pertussis, respectively. Methylation of these cells were compared to those of CD4⁺CD69⁺ T_{RM} isolated from Bm or Sp (Supporting information Fig. S9A). In total, 725 307 genomic tiles of 500 bp length were compared across all samples. Since epigenetic signatures of antigen-reactive memory T cells on d1 are expected to include both, circulating, antigen-reactive memory T cells already present on d0, and antigen-reactive T_{RM} mobilized from tissue, we focused on 10 632 tiles representing differentially methylated regions (DMR) with high variance (> 0.1) across the four sample types (Supporting information Fig. S9B). As such, DMR identified for T_{RM} of Bm and Sp, and antigen-reactive memory T cells of blood on d0 and d1, 85 signature

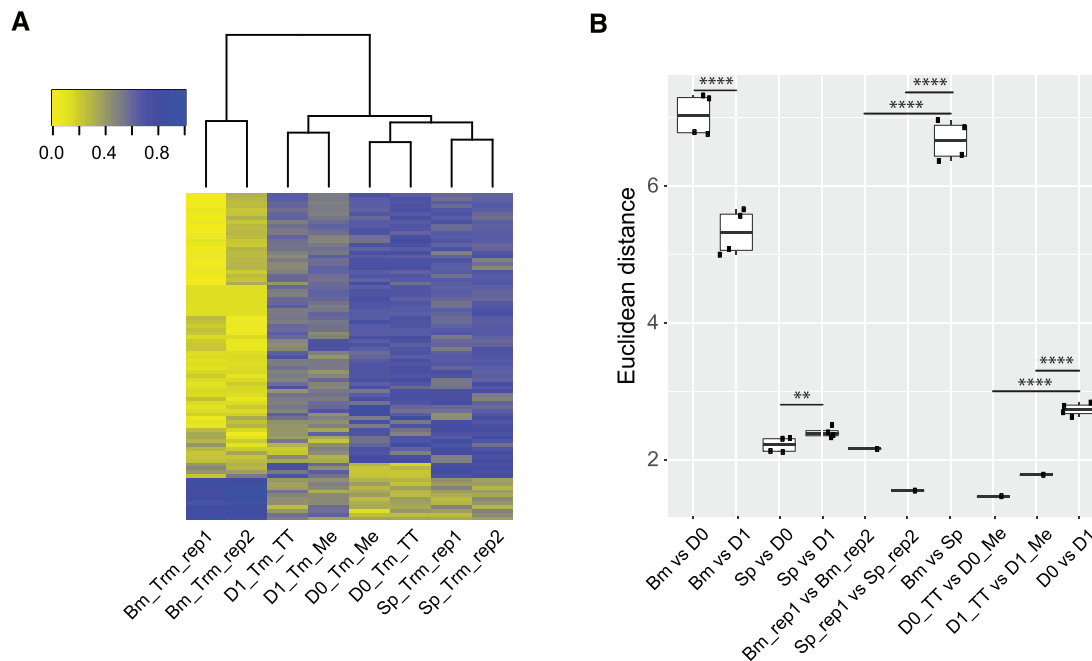


Figure 5. T_{RM} are mobilized from bone marrow. Antigen-reactive memory $CD4^+$ T cells before (D0) and after (D1) MMR or TT vaccination were isolated from two donors as described in Fig. 4. Methyomes of these cells were compared to those of $CD4^+CD69^+$ T_{RM} isolated from Bm or Sp, each two replicates, consisting of pooled cells from three individuals and/or cells from an individual (see also Supporting information Fig. S9A). (A) A heatmap of 85 identified signature DMR (see also Supporting information Fig. S9B) of 500-bp tile that are hypo- and hypermethylated for Bm versus Sp T_{RM} and overlap with those between D0 versus D1 cells were hierarchically clustered and displayed. The methylation beta value per tile is shown for each DMR in rows. The extent of methylation values is color coded. The more the yellow, the less the methylation value; the more the blue, the more the methylation value. (B) A Beeswarm boxplot based on the same DMR in (A). The value on the y-axis inversely correlates the similarity between two groups (e.g., Bm–D0) of each comparison listed on the x-axis. Distribution of the mean methylation beta values of all the DMR shown in (A) in cross comparisons of indicated samples. **** $p < 0.001$; ** $p < 0.01$. (A and B) Data shown are representative of at least four independent experiments.

DMR were identified (Supporting information Table S5). Among them, methylation of 74 DMR significantly hypomethylated and 11 DMR significantly hypermethylated in Bm as compared to Sp. The methylation pattern of those 85 DMR of circulating antigen-reactive memory T cells of d0 is similar to that of T_{RM} from Sp, less so to those from Bm. Antigen-reactive memory T cells of d1 present as intermediate between Sp and Bm, closer to Bm than those of d0, suggesting that antigen-reactive T_{RM} of d1 are a mixture of circulating memory T cells: those already present on d0 and previous T_{RM} mobilized from the Bm (Supporting information Fig. 5A). The change in similarity toward the Bm signature is highly significant ($p < 0.0001$; Fig. 5B). Moreover, we also compared the methylation patterns of those 85 DMR of these four analyzed cell types by principal component analysis. Corroborating the results shown in Fig. 5, the predominant principal component 1 (PC1, 83.345%) shows antigen-reactive memory T cells of d0 were more similar to Trm from Sp than from Bm, whereas antigen-reactive memory T cells of d1 moved away from Sp toward Bm. The PC2 (5.204%) also shows d1 cells were more close to Bm than Sp (Supporting information Fig. S8C). Taken together, the T_{RM} mobilized by vaccination show the epigenetic signatures of T_{RM} of the Bm, indicating that T_{RM} of the Bm can leave this tissue, circulate again and join immune reactions in secondary lymphoid organs.

Discussion

The discovery of memory T lymphocytes residing in distinct tissues, like the skin [2], lungs [4, 13] and Bm [7, 11] has revealed a considerable compartmentalization of immunological memory. T_{RM} lymphocytes, especially those residing in epithelial barrier tissues, have generally been considered to provide site-specific protection against repeated antigenic challenges within their tissue of residence [13, 18, 34]. The role of T_{RM} in systemic immune reactions of secondary lymphoid tissues has been enigmatic, despite the fact that more than 50 years ago, pioneering work by McGregor and Gowans had shown that, in the absence of circulating lymphocytes, secondary systemic immune reactions are not impaired [35]. Despite this fundamental observation, the contribution of T_{RM} to systemic secondary challenges has been, thus, far unexplored.

In the present study, we have tracked antigen-specific memory $CD4^+$ T lymphocytes in the peripheral blood of human adult donors over a 2-week time period following immunization with a combined MMR vaccine. All but one of the donors had pre-existing immunological memory for all of these viruses, that is, virus-specific IgG antibodies. In contrast to our previous cohort of 40–70 year old donors, most of whom did not have detectable numbers of measles-reactive memory $CD4^+$ T cells in the blood

[7], many of the present study subjects (aged 28–43 years) had detectable virus-reactive memory CD4⁺ T cells in the blood, before vaccination (d0). Irrespective of this, in 20 of the 29 secondary immune responses analyzed, we observed a rapid mobilization of virus-reactive memory CD4⁺ T cells into the blood, 16 to 24 h after immunization. These cells then disappeared from the blood between days 2 and 3, and reappeared again starting on day 7 and increasing in number until day 14, the last point of analysis. The rapid mobilization of CD4⁺ T_{RM} into the blood is antigen-specific (cognate), and contributes to the systemic immune response, as is evident by the presence of their antigen-specific clonotypes among those memory T cells isolated from blood samples taken on day 14. Interestingly, the mobilized T_{RM} show the epigenetic signature of T_{RM} of Bm, an organ which does not develop the germinal centers required for efficient secondary immune reactions in lymphoid tissue (Siracusa et al, 2018), while the antigen-specific circulating memory T cells of blood before vaccination resemble T_{RM} of the Sp.

Antigen-specific memory provided by the adaptive immune system is multilayered. Antibodies secreted by memory plasma cells provide immediate protection, while memory T and B lymphocytes provide reactive memory against excessive or modified antigen [9, 36]. Moreover, immune memory cells are compartmentalized in various tissues [9, 37]. We have previously shown that prominent populations of memory plasma cells and memory CD4⁺ and CD8⁺ T lymphocytes reside and rest in the Bm [7, 8, 11, 16]. Memory CD4⁺ T_{RM} of the Bm maintain long-term memory to systemic pathogens, like measles, mumps and rubella, even in the apparent absence of such memory cells circulating in the blood. CD4⁺ T_{RM} are heterogeneous, with a continuing debate on the transcriptional identity and lifestyle of these cells [7, 9, 10, 14, 16, 38]. Whether or not the residency is temporarily or longlasting, is not addressed here in detail, although our previous results, showing the exclusive presence of measles-reactive memory T cells in the Bm, as compared to the blood, would argue that the residency is longlasting, at least for measles-specific T_{RM} [7]. Here, we demonstrate the rapid mobilization of CD4⁺ T_{RM} specific for measles, mumps or rubella into the blood upon antigenic rechallenge, and describe their significant contribution to the systemic secondary immune response. The expression of CD154 on these cells and their rapid accumulation without proliferation indicates that they had been recently activated and mobilized. According to their epigenetic signature, T_{RM} of the Bm are mobilized, and these T_{RM} are polyfunctional in terms of cytokine expression, a decisive property of MMR-specific CD4⁺ T_{RM} of Bm [7].

Ten of the 11 immunized vaccinees (MMR1-3 and MMR5-11) had pre-existing memory to all three viruses. Only one donor, MMR4 did not have measles-specific IgG antibodies prior to vaccination. The 29 individual memory immune reactions analyzed in this study from the 11 donors who participated displayed a considerable amount of heterogeneity. For example, the rapid mobilization of virus-specific tissue-resident memory CD4⁺ T lymphocytes was independent of pre-existing antibody titers, for example, MMR6 and MMR8 both displayed rapid mobilization despite having dramatically different baseline antibody titers

against measles antigen (2408 and 424 mIU/mL, respectively). Mobilization of virus-specific tissue-resident memory CD4⁺ T cells also did not correlate with numbers of pre-existing circulating memory cells of the same specificity, for example, the number of mumps specific memory T cells per 10⁶ CD4⁺ T cells for MMR2 increased from 158 to 251 from d0 to d1, while in MMR5 numbers remained constant, 175 and 180, on d0 and d1. Moreover, mobilization of virus-specific tissue-resident memory CD4⁺ T cells did not correlate with the efficacy of generating new antigen-specific antibodies in the subsequent immune reaction (e.g., rubella titers in MMR2 remained stable, 142 before versus 140 U/mL following vaccination, while MMR3 showed an increase in rubella antibody titer from 82 to 140 U/mL) nor with increased numbers of antigen-specific memory T cells on day 14 (e.g., 1143 measles-specific memory T cells per 10⁶ CD4⁺ T cells measured from MMR2, and only 407 from MMR8). Thus, the mobilization of virus-specific T_{RM}, triggered by vaccination, is an independent event, and presumably reflects the availability of T_{RM} in a given vaccinee.

The mobilization of T_{RM} is cognate, that is, only antigen-reactive CD4⁺ T cells are mobilized. First of all, in the vaccinees analyzed, the overall numbers of memory CD4⁺ T lymphocytes in the blood did not change significantly after vaccination. Second, although we observed mobilization of memory CD4⁺ T cells recognizing TT, an antigen not present in the MMR vaccine, only TT-reactive CD4⁺ T cells that cross-react with the vaccine were mobilized, in line with the notion that mobilization is cognate. It might be due to the difference in time window of T-cell response assessed that others observed a bystander activation of pre-existing memory CD4⁺ T cells at week 1 or 2 post-TT vaccination [39, 40].

Rapid reactivation kinetics of T_{RM} has been observed within their host tissue previously. We have shown before, that in the maintenance phase of memory, T_{RM} of Bm individually localize to stromal cells of the Bm, and MHC class II-expressing APCs are not present within their vicinity [11, 25]. However, upon cognate reactivation in situ, T_{RM} of Bm are rapidly mobilized from their niches, aggregate in “immune clusters” with APCs and proliferate vigorously [25]. In the present study, mobilized CD4⁺ T_{RM} showed no sign of proliferation on day 1 and 2 after vaccination, suggesting that they had left their tissue niches and directly egressed into the blood, and not participated in the immune clusters of Bm.

In functional terms, the mobilized T_{RM} did contribute significantly to the subsequent systemic secondary immune reactions examined in our study. In the vaccinees analyzed, TCR clonotypes of mobilized T_{RM}, that is, those cells detected on day 1 but not on day 0, were present at equal or higher frequency among memory CD4⁺ T cells on day 14. In the relatively young population of vaccinees analyzed here (28- to 43-year-old), circulating memory CD4⁺ T cells and mobilized T_{RM} contributed about equally to the systemic secondary immune reaction. We have previously shown, in a cohort of subjects between 40 and 70 years of age, that circulating memory CD4⁺ T cells specific for measles, mumps, and rubella disappear, while their tissue-resident counterparts remain easily detectable in the Bm, which also hosts significant populations of memory T cells specific for other systemic pathogens

and antigens, for example, tetanus [7]. The present results would predict that in older individuals, the systemic secondary immune response to childhood pathogens is entirely dependent on the mobilization of T_{RM} . This would be predicted to provide efficient protection, due to the polyfunctional nature of these mobilized memory T cells [31].

Our results are in line with recent data obtained from animal models, demonstrating that T_{RM} can recirculate again and contribute to secondary immune reactions in secondary lymphoid tissues [26, 27]. Here, we demonstrate for the first time, that in humans, T_{RM} from the Bm, a tissue which does not develop GCs on its own, are mobilized in reaction to vaccination and participate significantly to secondary immune reactions. The Bm hosts significant numbers of memory T cells specific for systemic antigens, and obviously the immune system makes efficient use of them. This does not exclude the possibility that T_{RM} might be mobilized from other tissue(s) also hosting such long-term systemic T-cell memory, which has not yet been shown.

Materials and methods

Human Donors

The recruitment of study subjects was conducted in accordance with the approval from the local ethical commission Charité-Universitätsmedizin Berlin (EA1/303/12, EA1/105/09, and EA1/342/14) and informed consent in accordance with the Declaration of Helsinki. Sixteen healthy adults (5 males and 15 females; age \pm SEM = 34.29 ± 1.78) with either documented measles, mumps, or rubella vaccination history or exposure through natural measles, mumps, or rubella infection were screened for levels of pre-existing vaccine-reactive antibody titers (analyzed by Medizinisches Versorgungszentrum Labor, Berlin). The donor's previous antigen exposure, either by vaccination or by natural infection, was verified by detectable antigen-reactive antibody titers. This study discusses results obtained from seven donors without vaccination and 13 donors who received a live attenuated MMR (Priorix, GSK, Germany) or diphtheria-tetanus-pertussis (COVAXIS, Sanofi-Aventis, Germany) booster vaccination. Bm samples were obtained from six female donors (age \pm SEM = 65.4 ± 2.57) undergoing hip replacement operations. Sp cells were isolated from cryopreserved (-80°C) Sp tissue samples from four female donors (age \pm SEM = 44.5 ± 4.24) obtained for diagnostic purpose.

Sample collection and preparation

Fifty millilitres of blood was drawn from each donor before vaccination (day 0), and at six time points (16 h and days 1, 2, 3, 7, and 14) or at two time points (days 1 and 14) after vaccination into Vacutainer Heparin tubes (BD Biosciences, Plymouth, UK). Blood samples were subjected to immediate preparation and analyses.

Mononuclear cells were isolated by density gradient centrifugation using Ficoll-Hypaque (Sigma-Aldrich). Serum samples were collected on days 0, 1, 3, and 14 before and after vaccination into Vacutainer SSTTM tubes (BD Biosciences) and stored at -20°C until further use. Tissue-derived mononuclear cells were filtered with a $70\text{ }\mu\text{L}$ cell strainer prior to a density gradient centrifugation using Ficoll-Hypaque.

Flow cytometry analysis

Staining, data acquisition, and analysis were carried out as described previously [7, 41]. Eight- to twelve-color flow cytometry analysis was performed for the analysis of phenotype, cytokine profile, activation status, and cell sorting using a BD FACSaria cell sorter, LSRFortessa flow cytometer (BD Biosciences), or MACSQuant (Miltenyi Biotec). The following anti-human antibodies were used to stain cells: CD45, CD3, CD19, CD14, CD4, CD8, CD45RA, CD25, CD127, CCR7, Ki67, CD154, CD69, IFN- γ , IL-2, TNF α , and fixable live/dead or PI. Stained cells were acquired using FACSDiva (BD Biosciences) or MACSQuantify software and data were analyzed with FlowJo (Tree Star).

Quantification of leukocytes

Immediately following each blood draw, a $50\text{ }\mu\text{L}$ aliquot of whole blood was stained with $50\text{ }\mu\text{L}$ of a fluorochrome-conjugated mouse anti-human antibody mixture (CD45, CD56, CD19, CD14, CD3, CD4, and CD8) in the presence of FcR-blocking reagent (1:5). After staining, erythrocytes were lysed by adding $500\text{ }\mu\text{L}$ of buffer EL and incubating for 30 min at 4°C . A $300\text{ }\mu\text{L}$ of each sample was acquired and the total number of CD3⁺THcells was enumerated on a MACSQuant (Miltenyi Biotec) and used to estimate the number of CD4⁺CD45RA⁺ memory T cells according to the frequency of CD45RA⁺ among CD4⁺ cells in the staining panel of analyzing antigen-reactive memory CD4⁺ T cells.

Identification of antigen-reactive memory CD4⁺ T cells

PBMCs were cultured in RPMI 1640 supplemented with 1% GlutaMAX, 100 U/mL penicillin, 100 $\mu\text{g/mL}$ streptomycin, and 5% (vol/vol) human AB serum. Anti-CD28 (1 $\mu\text{g/mL}$), measles (5 $\mu\text{g/mL}$), mumps (10 $\mu\text{g/mL}$), rubella (5 $\mu\text{g/mL}$) antigen, and TT (1 lethal factor/mL) were used to stimulate cells. Stimulation with CD28 alone and in combination with *Staphylococcal enterotoxin B* (1 $\mu\text{g/mL}$) were used as negative and positive controls, respectively. For each condition, at least $5\text{--}10 \times 10^6$ cells were stimulated for a total of 7 h at 37°C and 5% CO_2 , with brefeldin A (1 $\mu\text{g/mL}$) added to the mixture for the last 4 h. Stimulated cells were first stained for surface antigens followed by fixation with BD FACS lysing and Perm2 solutions according to the manufacturer's instruction. Antigen-reactive memory CD4⁺ T cells were identified as Live/Dead⁺CD19⁺CD14⁺CD3⁺CD8⁺CD4⁺

CD45RA⁺CD154⁺cytokine⁺ and proliferating antigen-reactive cells as live/dead⁺CD19⁺CD14⁺CD3⁺CD8⁺CD4⁺CD45RA⁺CD154⁺Ki67⁺. At least 10⁶ lymphocytes were analyzed for each condition. Additionally, antigen-reactive CD154⁺ memory CD4⁺ cells were isolated using the CD154 MicroBead Kit. In brief, cells were labeled with CD154-biotin conjugated antibodies before incubation with anti-biotin microbeads and enriched by two sequential MS MACS columns. Cell surface staining was performed on the first column, followed by fixation, permeabilization, and intracellular cytokine staining on the second column using a previously established protocol [28].

Isolation of antigen-reactive memory CD4⁺ T cells

At least 5 × 10⁶ PBMCs were stimulated for 7 h with antigen in the presence of 1 µg/mL anti-CD40. Stimulated cells were stained for 15 min at room temperature with the following antibodies: CD3, CD4, CD8, CD19, CD14, CD45RA, CD69, and CD154. Antigen-reactive memory CD4⁺ T cells were identified by the expression of PI⁺CD19⁺CD14⁺CD3⁺CD8⁺CD4⁺CD45RA⁺CD154⁺CD69⁺. Measles-reactive memory CD4⁺ T cells sorted before, days 1 and 14 after vaccination were further processed for TCR CDR3 Vβ sequencing. In addition, measles- and TT-reactive memory CD4⁺ T cells sorted 1 day after vaccination were used for the generation of antigen-reactive T-cell lines.

Expansion and restimulation of antigen-reactive memory CD4⁺ T-cell lines

Purified antigen-reactive CD69⁺CD154⁺ memory CD4⁺ T cells (as described earlier) were cultured with CD3 depleted and irradiated (40 Gy on ice for 35 min) autologous feeder cells at ratios of 1:100 in a 48-well plate in X-VIVO15 medium supplemented with 100 U/mL penicillin, 100 µg/mL streptomycin, 5% (vol/vol) human AB serum, and 200 IU/mL IL-2. Cells were expanded for 14 days, with 200 IU/mL IL-2 supplemented every 3 days during the first 10 days of the cell culture.

For restimulation, freshly isolated autologous PBMCs were labeled with CFSE (1 µM) following the manufacturer's protocol. CFSE-labeled PBMCs were cocultured with 2.5 × 10⁵ expanded T cells at ratios of 2:1 and stimulated with different antigens (measles, mumps, rubella, TT, or CMV) in the presence of CD28 (1 µg/mL) for 6 h, with the last 4 h with brefeldin A (1 µg/mL). Stimulated cells were stained with surface antigens and intracellular cytokines.

Determination of antigen-specific antibodies by Enzyme-linked Immunosorbent Assay (ELISA)

Before and after MMR vaccination, antigen specific IgG responses against measles, mumps, or rubella, using an antigen-specific ELISA kit following the manufacturer's recommendations. Sim-

ilarly, levels of serum IgG against TT were analyzed with an antigen-specific ELISA kit.

TCR CDR3 Vβ gene library preparation

Total RNA was extracted from 2500 measles-reactive memory CD4⁺ T cells using the Qiazol Lysis Reagent and a miRNAeasy Micro Kit, following the manufacturer's protocols. The resulting 13 µL RNA was assayed for concentration and quality using a Bioanalyzer. Eight microliter RNA was then processed for TCR CDR3 Vβ library preparation, following a published protocol [42] with modifications. Briefly, the first strand of cDNA with the 5' template switch adapter SmartNNNa was synthesized using a SMARTScribe reverse transcriptase, following the manufacturer's instruction. cDNAs were purified using a MinElute PCR purification Kit prior to a two-step PCR with a proof-reading Q5 DNA polymerase and barcoded primers (see key resources table). PCR products from each step were purified using a QIAquick PCR purification kit, following manufacturer's instruction. Second round of PCR products containing fragments (about 550 bp in length) were sliced under a Blue LED Transilluminator (Herolab, Germany) and further purified by PCR-clean-up gel extraction and stored at −20°C until adaptor ligation and sequencing. The concentration of the size-selected PCR products was determined using a Qubit fluorometer. Finally, all barcoded PCR products or samples were mixed together at equal ratios, and the Illumina adapters were ligated according to the manufacturer's protocol. Pooled libraries were purified by PCR-clean-up gel extraction.

TCR CDR3 Vβ gene sequencing and data analysis

Paired-end (2 × 150 bp) sequencing of the TCR CDR3 Vβ gene transcripts were performed on an Illumina NextSeq 500 platform. Inline barcodes were demultiplexed and the Illumina adapters removed by Illumina's bcl2fastq 1.8.4 software. Demultiplexing of sample barcodes as well as the extraction of the CDR3 Vβ gene sequences were performed by the open source software tools mige 1.2.4 [43] and VDJtools [43] using the unique molecular identifier (UMI)-guided assembling and error correction with default setting, minimal number of 5 reads per UMI and blast. Data from two replicates at the same time point were either pooled or merged for overlap if specified. For downstream analysis and plotting, base-level R functions and the public available software package VDJtools [44] were used.

The inverse Simpson index is a measure of diversity commonly applied in ecology, it can be computed as $D = \left[\sum_{i=1}^n p_i^2 \right]^{-1}$, where the p_i are relative frequencies of all n observed clonotypes. If all clonotypes have equal frequency, that is, $p_i = 1/n$ for all i , then $D = n$, and, therefore, D can be interpreted as the "effective number of parties" generating the observed diversity in a given sample. Although the inverse Simpson index is a

comparatively robust measure of diversity [32], for direct comparisons between experiments we adjusted the total number of reads by “downsampling,” that is, taking a random selection of samples until the number of reads in the smallest sample is reached.

Isolation of CD4⁺ T_{RM} from Bm and Sp samples

Single-cell suspension of Bm and Sp samples was stained with surface antibodies for 10 min at 4°C. DAPI (1 µg/mL) was used as a dead cell exclusion marker. Viable T_{RM} (CD4⁺CD69⁺ memory T-cells) were purified as CD45⁺CD3⁺DUMP[−]CD25[−]CD4⁺CD45RO⁺CD69⁺ by FACS using a BD FACSAria II cell sorter (BD Biosciences). Purity of the sorted cells was determined as >98% by postsort check. Data were analyzed using the FlowJo V10 software (Tree Star).

Genomic DNA extraction and mRRBS

Purified T_{RM} cells from Bm and Sp samples, and blood antigen-reactive memory CD4⁺ T cells isolated before (d0) and after (d1) MMR or TT vaccination were immediately subject to genomic (g) DNA extraction using a DNeasy blood and tissue kit (Qia-gen), following the manufacturer's protocol. All gDNA samples were quantified using a Qubit fluorometer (Invitrogen). Six DNA samples were pooled into two DNA samples (each pool consists of equal amount of gDNA purified from the identical cell type of three female donors). mRRBS was applied for higher throughput and low amounts of input DNA according to the published procedure 2 [45], with minor modifications. Briefly, 50–100 ng of gDNA was digested overnight at 37°C with *Hae*III restriction enzyme in a 30-µL reaction. After A-tailing reaction with Klenow fragment exo-, sample-specific sequencing adaptors were ligated using T4-ligase followed by bisulfite conversion with the EZ-DNA methylation Gold kit and 12–18 cycles of PCR amplification. After purification with AMPure XP beads, libraries went through quality checks (qPCR and Agilent Bioanalyzer) and were sequenced 1 × 100 single read on an Illumina HiSeq 2500 machine.

Mapping of mRRBS data

Generated mRRBS raw data were decoded with GenomeStudio software (Illumina) and then processed as described previously [24, 46]. The reads were aligned to the 1000 genomes version of the human hg38 reference [47] using the BWA (v0.6.2) [48], and the wrapper methylTools (v0.9.2), Samtools (v1.3) [49], and Picard tools (v1.115) (“Picard Tools-By Broad Institute” 2017) for converting, merging, and indexing of alignment files. Bis-SNP was used for SNP (dbSNP, v138, National Center for Biotechnology Information, National Library of Medicine 2013) aware realignment, quality recalibration, and methylation calls.

Calling of DNA-methylation values and identification of DMR

Beta-values of 500-bp genomic tiles of memory CD4⁺ T cells isolated from the Bm (2 pools), Sp (1 pool plus 1 individual), and vaccine samples of days 0 and 1 (each time point from the same two individuals) were calculated using R (version 3.6.3) and MethyKit package [50]. The raw data of Bm pool 1 were taken from the European Genome-Phenome Archive under the accession number EGAS0000100624 [24]. In total, beta-values of 7 25 307 tiles were calculated and reduced using five different filtering steps to identify four categories of small tile subsets of Bm-hypo, Bm-hyper, Sp-hypo, and Sp-hyper which might hint at the origin of mobilized T_{RM} in D1 cells, that is, D0 cells mixed with T_{RM} mobilized from Bm and/or Sp.

We first filtered out all tiles with a variance >0.1 across all samples (step 1) for data set 2, by applying a numeric gradient filter from the highest to the lowest beta-values in 24 permutations of four sample groups Bm, Sp, D0, and D1 (step 2). We next determined the shared tiles in intersection of the top 90% highest ranked tiles in variance between Bm and Sp (Bm vs. Sp) and between D0 and D1 (D0 vs. D1) for 24 different data sets 4 (step 3). Subsequently, we filtered out tiles with intragroup variance <0.1 in the Bm, Sp, D0, and D1 samples and a methylation difference >50% for Bm versus Sp in beta mean values and >10% for D0 versus D1 in beta mean values to obtain 24 data sets 5 as potential methylome signatures (step 4).

To estimate the similarities between sample groups, we then calculated the Euclidean distance values of tiles determined in the 24 data sets 5. The following groups were compared: Bm versus D0, Bm versus D1, Sp versus D0, Sp versus D1, (Bm vs. Sp) versus Bm(rep)1_Bm2, (Bm vs. Sp) versus Sp1_Sp2, (D0 vs. D1) versus D0_(rep)1_D0_2, and (D0 vs. D1) versus D1_1_D1_2. The smaller the Euclidean distance value in a comparison, the more similar the samples are in that comparison. The Euclidean distance values were visualized in Beeswarm plots.

We ultimately reduced the 24 data set 5 to only four data sets 5 (combined to data set 6). In these four data sets 5, the Euclidean distance values for the intergroup comparison (Bm vs. Sp; D0 vs. D1) were significantly higher than for intragroup comparisons (i.e., Bm1 vs. Bm2 and Sp1 vs. Sp2; D0_1 vs. D0_2, and D1_1 vs. D1_2) (step 5).

The remaining 18 data sets 5 were not considered as they do not address our hypothesis. In brief, in eight data sets 5 no tiles were called (case 1). In another six data sets 5, the Euclidean distance values between the intergroup comparisons versus intragroup comparisons were not significant (case 2). Finally, additional four data sets 5 either showed greater Euclidean distance values for Bm versus D1 compared to Bm versus D0 (case 3) or for Sp versus D1 compared to Sp versus D0 (case 4), respectively.

In case 1, the similarity of D1 to Bm or Sp cannot be calculated as no tiles were recovered. In case 2, the similarity of D1 to Bm or Sp cannot be judged as Euclidean distance values for the intergroup comparisons and the intragroup comparisons are not well separated from each other. Case 3 suggested that D1 became

more dissimilar to Bm and did not change its similarity to Sp. Case 4 suggested that D1 became more dissimilar to Sp and did not change similarity to Bm.

To answer the question whether D1 becomes more similar to Bm or Sp after vaccination, we need to detect a decrease in Euclidean distance values of Bm versus D1 compared to Bm versus D0 and/or Sp versus D1 compared to Sp versus D0.

If there are no changes or even an increase in the Euclidean distance values in Bm versus D1 or Sp versus D1 as seen in cases 3 and 4, respectively, these four data sets 5 did not reveal any further information whether D1 becomes more similar to Bm and/or Sp after vaccination. Thus, the four data sets 5 of cases 3 and 4 were excluded from data set 6, resulting in the data set 6 consisting of only four remaining data sets 5.

The one-sided *p*-values in Beeswarm plots were calculated using the cumulative distribution function for normal distribution implemented as *pnorm* function in R.

Quantification and statistical analyses

Polyfunctionality of antigen-reactive memory CD4⁺ T cells was analyzed using Flowjo Boolean (logic) operators (AND and NOT) for overlapping regions to define all possible combinations of cytokine profiles. The results were displayed as the absolute number of cytokine-producing cells per 10⁶ CD4⁺ T cells or per 10³ CD154 MACS enriched cells.

Statistical analyses for differences in antigen-reactive memory CD4⁺ T cells induced by MMR vaccination were performed by one-tailed paired *t*-test to test for an early increase of T-cell numbers in individual donors.

Comparison of intersections of TCR repertoire samples after repetitive downsampling was performed using a rank-based permutation test (method “oneway” from the R-based “coin” package).

In all analyses, *p*-values ≤ 0.05 were considered to be statistically significant.

Contact for reagent and resource sharing

Detailed reagents and resources are available in Supporting information Table S6. Further information and requests for resources and reagents should be directed to and will be fulfilled by the Lead Contact, Dr. Jun Dong (dong@drfz.de). This study did not generate new unique reagents.

Acknowledgments: This work was supported by the Deutsche Forschungsgemeinschaft (DFG, German Research Foundation)–Projektnummer 389687267 awarded to JD and AR, in part by the European Research Council (ERC) Advanced Grant 268987 (to

AR), and by the Chinesisch-Deutsches Zentrum für Wissenschaftsförderung (Sino-German Center for Research Promotion (SGC); DFG im Ausland)–Grant C-0072 awarded to JD. CC was supported in part by the Leibniz Graduate School for Rheumatology (LGRh). WD was supported in part by the China Scholarship Council (CSC). HDC was supported by the Dr. Rolf M. Schwiete Foundation. MFM was supported by the state of Berlin and the “European Regional Development Fund” (ERDF 2014–2020, EFRE 1.8/11, Deutsches Rheuma-Forschungszentrum). KT was supported by “Best minds” program of the Leibniz association. JD was supported in part by the Leibniz science Campus Chronic Inflammation (www.chronische-entzuendung.org).

Conflict of interest: The authors declare no conflict of interest.

Ethics approval and patient consent statement: The recruitment of study subjects was conducted in accordance with the approval from the local ethical commission Charité–Universitätsmedizin Berlin (EA1/303/12, EA1/105/09, and EA1/342/14) and informed consent in accordance with the Declaration of Helsinki.

Author contributions: Conceptualization, JD and AR; Methodology, CC, WD, and JD; Investigation, CC, WD, A Rao, GG, GAH and MFM.; Formal Analysis, WD, CC, PD, YCL, XY, AS, KN, TL, KT, and JD; Data curation, PD, YCL, XY, AS, KN, TL, and KT; Resources, TA, ARS, ALS, TD, AC, KS, HDC, HDV, CR, ZQ, SH, CK, SR, and JW; Interpretation, CC, WD, AR and JD; Writing – Original Draft, JD; Writing – Review & Editing, LS, KT, AR, and JD; Visualization, WD, YCL, KT, and JD; Supervision, JD; Project Administration, JD; Funding Acquisition, JD and AR. All authors contributed to the final version of the manuscript.

Data availability statement: The TCR CDR3 Vβ gene sequencing datasets generated during this study have been deposited in the Gene Expression Omnibus (GEO) database (www.ncbi.nlm.nih.gov/geo) with the accession number GSE151738 and will be available from the date of publication. The methylomes generated during this study have been deposited in the European Genome-Phenome Archive (EGA) with the accession number EGAS00001005475 (<https://ega-archive.org/>) and are available from the corresponding author upon reasonable request.

Peer review: The peer review history for this article is available at <https://publons.com/publon/10.1002/eji.202149726>.

References

- 1 Sallusto, F., Lenig, D., Förster, R., Lipp, M. and Lanzavecchia, A., Two subsets of memory T lymphocytes with distinct homing potentials and effector functions. *Nature* 1999. 401: 708–712.
- 2 Gebhardt, T., Wakim, L. M., Eidsmo, L., Reading, P. C., Heath, W. R. and Carbone, F. R., Memory T cells in nonlymphoid tissue that provide enhanced local immunity during infection with herpes simplex virus. *Nat. Immunol.* 2009. 10: 524–530.

- 3 Clark, R. A., Watanabe, R., Teague, J. E., Schlapbach, C., Tawa, M. C., Adams, N., Dorosario, A. A., et al., Skin effector memory T cells do not recirculate and provide immune protection in alemtuzumab-treated CTCL patients. *Sci. Transl. Med.* 2012. **4**: 117ra7.
- 4 Kumar, B. V., Ma, W., Miron, M., Granot, T., Guyer, R. S., Carpenter, D. J., Senda, T., et al., Human tissue-resident memory T cells are defined by core transcriptional and functional signatures in lymphoid and mucosal sites. *Cell Rep.* 2017. **20**: 2921–2934.
- 5 Purwar, R., Campbell, J., Murphy, G., Richards, W. G., Clark, R. A. and Kupper, T. S., Resident memory T cells (T(RM)) are abundant in human lung: diversity, function, and antigen specificity. *PLoS One* 2011. **6**: e16245.
- 6 Stelma, F., de Niet, A., Sinnige, M. J., van Dort, K. A., van Gisbergen, K. P. J. M., Verheij, J., van Leeuwen, E. M. M., et al. Human intrahepatic CD69 + CD8+ T cells have a tissue resident memory T cell phenotype with reduced cytolytic capacity. *Sci. Rep.* 2017. **7**: 6172.
- 7 Okhrimenko, A., Grün, J. R., Westendorf, K., Fang, Z., Reinke, S., Von Roth, P., Wassilew, G., et al., Human memory T cells from the bone marrow are resting and maintain long-lasting systemic memory. *Proc. Natl. Acad. Sci. U.S.A.* 2014. **111**: 9229–9234.
- 8 Sercan Alp, Ö., Durlanik, S., Schulz, D., Mcgrath, M., Grün, J. R., Bardua, M., Ikuta, K., et al., Memory CD8+ T cells colocalize with IL-7+ stromal cells in bone marrow and rest in terms of proliferation and transcription. *Eur. J. Immunol.* 2015. **45**: 975–987.
- 9 Chang, H.-D., Tokoyoda, K. and Radbruch, A., Immunological memories of the bone marrow. *Immunol. Rev.* 2018. **283**: 86–98.
- 10 Siracusa, F., Alp, Ö. S., Maschmeyer, P., Mcgrath, M., Mashregi, M.-F., Hojyo, S., Chang, H.-D., et al., Maintenance of CD8(+) memory T lymphocytes in the spleen but not in the bone marrow is dependent on proliferation. *Eur. J. Immunol.* 2017. **47**: 1900–1905.
- 11 Tokoyoda, K., Zehentmeier, S., Hegazy, A. N., Albrecht, I., Grün, J. R., Löhning, M. and Radbruch, A., Professional memory CD4+ T lymphocytes preferentially reside and rest in the bone marrow. *Immunity* 2009. **30**: 721–730.
- 12 Steinert, E. M., Schenkel, J. M., Fraser, K. A., Beura, L. K., Manlove, L. S., Igyártó, B. Z., Southern, P. J., et al., Quantifying memory CD8 T cells reveals regionalization of immunosurveillance. *Cell* 2015. **161**: 737–749.
- 13 Tejaro, J. R., Turner, D., Pham, Q., Wherry, E. J., Lefrançois, L. and Farber, D. L., Cutting edge: tissue-retentive lung memory CD4 T cells mediate optimal protection to respiratory virus infection. *J. Immunol.* 2011. **187**: 5510–5514.
- 14 Mackay, L. K., Minnich, M., Kragten, N. A. M., Liao, Y., Nota, B., Seillet, C., Zaid, A., et al., Hobit and Blimp1 instruct a universal transcriptional program of tissue residency in lymphocytes. *Science* 2016. **352**: 459–463.
- 15 Shinoda, K., Tokoyoda, K., Hanazawa, A., Hayashizaki, K., Zehentmeier, S., Hosokawa, H., Iwamura, C., et al., Type II membrane protein CD69 regulates the formation of resting T-helper memory. *Proc. Natl. Acad. Sci.* 2012. **109**: 7409–7414.
- 16 Siracusa, F., Durek, P., Mcgrath, M. A., Sercan-Alp, Ö., Rao, A., Du, W., Cendón, C., et al., CD69(+) memory T lymphocytes of the bone marrow and spleen express the signature transcripts of tissue-resident memory T lymphocytes. *Eur. J. Immunol.* 2019. **49**, 966–968.
- 17 Jiang, X., Clark, R. A., Liu, L., Wagers, A. J., Fuhlbrigge, R. C. and Kupper, T. S., Skin infection generates non-migratory memory CD8+ T(RM) cells providing global skin immunity. *Nature* 2012. **483**: 227–231.
- 18 Mackay, L. K., Stock, A. T., Ma, J. Z., Jones, C. M., Kent, S. J., Mueller, S. N., Heath, W. R., et al., Long-lived epithelial immunity by tissue-resident memory T (TRM) cells in the absence of persisting local antigen presentation. *Proc. Natl. Acad. Sci. U.S.A.* 2012. **109**: 7037–7042.
- 19 Watanabe, R., Gehad, A., Yang, C., Scott, L. L., Teague, J. E., Schlapbach, C., Elco, C. P., et al., Human skin is protected by four functionally and phenotypically discrete populations of resident and recirculating memory T cells. *Sci. Transl. Med.* 2015. **7**: 279ra39.
- 20 Hogan, R. J., Zhong, W., Usherwood, E. J., Cookenham, T., Roberts, A. D. and Woodland, D. L., Protection from respiratory virus infections can be mediated by antigen-specific CD4(+) T cells that persist in the lungs. *J. Exp. Med.* 2001. **193**: 981–986.
- 21 Dong, J., Chang, H.-D., Ivancu, C., Qian, Y., Rezai, S., Okhrimenko, A., Cosmi, L., et al., Loss of methylation at the IFNG promoter and CNS-1 is associated with the development of functional IFN-gamma memory in human CD4(+) T lymphocytes. *Eur. J. Immunol.* 2013. **43**: 793–804.
- 22 Tykocinski, L.-O., Hajkova, P., Chang, H.-D., Stamm, T., Sözeri, O., Löhning, M., Hu-Li, J., et al., A critical control element for interleukin-4 memory expression in T helper lymphocytes. *J. Biol. Chem.* 2005. **280**: 28177–28185.
- 23 Mazzoni, A., Santarlasci, V., Maggi, L., Capone, M., Rossi, M. C., Querci, V., De Palma, R., et al., Demethylation of the RORC2 and IL17A in human CD4+ T lymphocytes defines Th17 origin of nonclassic Th1 cells. *J. Immunol.* 2015. **194**: 3116–3126.
- 24 Durek, P., Nordström, K., Gasparoni, G., Salhab, A., Kressler, C., De Almeida, M., Bassler, K., et al., Epigenomic profiling of human CD4+ T cells supports a linear differentiation model and highlights molecular regulators of memory development. *Immunity* 2016. **45**: 1148–1161.
- 25 Siracusa, F., Mcgrath, M. A., Maschmeyer, P., Bardua, M., Lehmann, K., Heinz, G., Durek, P., et al., Nonfollicular reactivation of bone marrow resident memory CD4 T cells in immune clusters of the bone marrow. *Proc. Natl. Acad. Sci. U.S.A.* 2018. **115**, 1334–1339.
- 26 Behr, F. M., Parga-Vidal, L., Kragten, N. A. M., Van Dam, T. J. P., Wesselink, T. H., Sheridan, B. S., Arens, R., et al., Tissue-resident memory CD8(+) T cells shape local and systemic secondary T cell responses. *Nat. Immunol.* 2020. **21**: 1070–1081.
- 27 Fonseca, R., Beura, L. K., Quarnstrom, C. F., Ghoneim, H. E., Fan, Y., Zebiley, C. C., Scott, M. C., et al., Developmental plasticity allows outside-in immune responses by resident memory T cells. *Nat. Immunol.* 2020. **21**: 412–421.
- 28 Bacher, P., Schink, C., Teutschbein, J., Kniemeyer, O., Assenmacher, M., Brakhage, A. A. and Scheffold, A., Antigen-reactive T cell enrichment for direct, high-resolution analysis of the human naive and memory Th cell repertoire. *J. Immunol.* 2013. **190**: 3967–3976.
- 29 Gerdes, J., Schwab, U., Lemke, H. and Stein, H., Production of a mouse monoclonal antibody reactive with a human nuclear antigen associated with cell proliferation. *Int. J. Cancer* 1983. **31**: 13–20.
- 30 Betts, M. R., HIV nonprogressors preferentially maintain highly functional HIV-specific CD8+ T cells. *Blood* 2006. **107**: 4781–4789.
- 31 Seder, R. A., Darrah, P. A. and Roederer, M., T-cell quality in memory and protection: implications for vaccine design. *Nat. Rev. Immunol.* 2008. **8**: 247–258.
- 32 Miho, E., Yermanos, A., Weber, C. R., Berger, C. T., Reddy, S. T. and Greiff, V., Computational strategies for dissecting the high-dimensional complexity of adaptive immune repertoires. *Front. Immunol.* 2018. **9**: 224.
- 33 Meissner, A., Reduced representation bisulfite sequencing for comparative high-resolution DNA methylation analysis. *Nucleic. Acids. Res.* 2005. **33**: 5868–5877.
- 34 Hofmann, M., Oschowitz, A., Kurzhals, S. R., Krüger, C. C., Pircher, H., et al., Thymus-resident memory CD8+T cells mediate local immunity. *Eur. J. Immunol.* 2013. **43**: 2295–2304.
- 35 McGregor, D. D. and Gowans, J. L., The antibody response of rats depleted of lymphocytes by chronic drainage from the thoracic duct. *J. Exp. Med.* 1963. **117**: 303–320.

- 36 Ahmed, R. and Gray, D., Immunological memory and protective immunity: understanding their relation. *Science* 1996. **272**: 54–60.
 - 37 Farber, D. L., Yudanin, N. A. and Restifo, N. P., Human memory T cells: generation, compartmentalization and homeostasis. *Nat. Rev. Immunol.* 2014. **14**: 24–35.
 - 38 Szabo, P. A., Levitin, H. M., Miron, M., Snyder, M. E., Senda, T., Yuan, J., Cheng, Y. L., Bush, E. C., Dogra, P., Thapa, P., Farber, D. L. and Sims, P. A., Single-cell transcriptomics of human T cells reveals tissue and activation signatures in health and disease. *Nat. Commun.* 2019. **10**: 4706.
 - 39 Li Causi, E., Parikh, S. C., Chudley, L., Layfield, D. M., Ottensmeier, C. H., Stevenson, F. K. and Di Genova, G., Vaccination expands antigen-specific CD4+ memory T cells and mobilizes bystander central memory T cells. *PLoS One* 2015. **10**: e0136717.
 - 40 Genova, G. D., Roddick, J., McNicholl, F. and Stevenson, F. K., Vaccination of human subjects expands both specific and bystander memory T cells but antibody production remains vaccine specific. *Blood* 2006. **107**: 2806–2813.
 - 41 Cossarizza, A., Chang, H.-D., Radbruch, A., Abrignani, S., Addo, R., Akdis, M., Andrä, I., et al., Guidelines for the use of flow cytometry and cell sorting in immunological studies (third edition). *Eur. J. Immunol.* 2021. **51**: 2708–3145.
 - 42 Mamedov, I. Z., Britanova, O. V., Zvyagin, I. V., Turchaninova, M. A., Bolotin, D. A., Putintseva, E. V., Lebedev, Y. B., et al., Preparing unbiased T cell receptor and antibody cDNA libraries for the deep next generation sequencing profiling. *Front. Immunol.* 2013. **4**.
 - 43 Shugay, M., Britanova, O. V., Merzlyak, E. M., Turchaninova, M. A., Mamedov, I. Z., Tuganbaev, T. R., Bolotin, D. A., et al., Towards error-free profiling of immune repertoires. *Nat Meth* 2014. **11**: 653–655.
 - 44 Shugay, M., Bagaev, D. V., Turchaninova, M. A., Bolotin, D. A., Britanova, O. V., Putintseva, E. V., Pogorelyy, M. V., et al., VDJtools: unifying post-analysis of T cell receptor repertoires. *PLoS Comput. Biol.* 2015. **11**: e1004503.
 - 45 Boyle, P., Clement, K., Gu, H., Smith, Z. D., Ziller, M., Fostel, J. L., Holmes, L., et al., Gel-free multiplexed reduced representation bisulfite sequencing for large-scale DNA methylation profiling. *Genome Biol.* 2012. **13**: 1–10.
 - 46 Wang, T., Liu, Q., Li, X., Wang, X., Li, J., Zhu, X., Sun, Z. S. and Wu, J., RRBS-A nalyser: a comprehensive web server for reduced representation bisulfite sequencing data analysis. *Human Mutat.* 2013. **34**: 1606–1610.
 - 47 Auton, A., Abecasis, G. R., Altshuler, D. M., Durbin, R. M., Abecasis, G. R., Bentley, D. R., Chakravarti, A., et al., A global reference for human genetic variation. *Nature* 2015. **526**: 68.
 - 48 Li, H. and Durbin, R., Fast and accurate long-read alignment with Burrows–Wheeler transform. *Bioinformatics* 2010. **26**: 589–595.
 - 49 Li, H., Handsaker, B., Wysoker, A., Fennell, T., Ruan, J., Homer, N., Marth, G., Abecasis, G., et al., The sequence alignment/map format and SAMtools. *Bioinformatics* 2009. **25**: 2078–2079.
 - 50 Akalin, A., Kormaksson, M., Li, S., Garrett-Bakelman, F. E., Figueroa, M. E., Melnick, A. and Mason, C. E., methylKit: a comprehensive R package for the analysis of genome-wide DNA methylation profiles. *Genome Biology* 2012. **13**: 1–9.
- Abbreviations:** **T_{RM}**: tissue-resident memory T cells · **T_{EM}**: effector memory T cells · **T_{CM}**: central memory T cells · **MMR**: measles-mumps-rubella · **TT**: tetanus toxoid · **TCR**: T-cell receptor · **mRRBS**: multiplex reduced representation of bisulfite sequencing · **DMR**: differentially methylated regions · **Sp**: spleen
- Full correspondence:** Dr. Jun Dong, Cell Biology Group, Deutsches Rheuma-Forschungszentrum Berlin (DRFZ), an Institute of the Leibniz Association, Charitéplatz 1, 10117, Berlin, Germany.
e-mail: dong@drfz.de
- Received: 11/11/2021
Revised: 27/1/2022
Accepted: 1/3/2022
Accepted article online: 4/3/2022